Measurement of transmission efficiency for 400 MeV proton beam through collimator at Fermilab MuCool Test Area using Chromox-6 scintillation screen

M. R. Jana, M. Chung, B. Freemire, P. Hanlet, M. Leonova, A. Moretti, M. Palmer, T. Schwarz, A. Tollestrup, Y. Torun, and K. Yonehara

Citation: Review of Scientific Instruments **84**, 063301 (2013); doi: 10.1063/1.4808275
View online: http://dx.doi.org/10.1063/1.4808275
View Table of Contents: http://scitation.aip.org/content/aip/journal/rsi/84/6?ver=pdfcov
Published by the AIP Publishing

Measurement of transmission efficiency for 400 MeV proton beam through collimator at Fermilab MuCool Test Area using Chromox-6 scintillation screen

M. R. Jana,[1,a)] M. Chung,[1,b)] B. Freemire,[2] P. Hanlet,[2] M. Leonova,[1] A. Moretti,[1] M. Palmer,[1] T. Schwarz,[1] A. Tollestrup,[1] Y. Torun,[2] and K. Yonehara[1]
[1]*Fermi National Accelerator Laboratory, Batavia, Illinois 60510, USA*
[2]*Illinois Institute of Technology, Chicago, Illinois 60616, USA*

(Received 19 March 2013; accepted 18 May 2013; published online 7 June 2013)

The MuCool Test Area (MTA) at Fermilab is a facility to develop the technology required for ionization cooling for a future Muon Collider and/or Neutrino Factory. As part of this research program, feasibility studies of various types of RF cavities in a high magnetic field environment are in progress. As a unique approach, we have tested a RF cavity filled with a high pressure hydrogen gas with a 400 MeV proton beam in an external magnetic field (B = 3 T). Quantitative information about the number of protons passing through this cavity is an essential requirement of the beam test. The MTA is a flammable gas (hydrogen) hazard zone. Due to safety reasons, no active (energized) beam diagnostic instrument can be used. Moreover, when the magnetic field is on, current transformers (toroids) used for beam intensity measurements do not work due to the saturation of the ferrite material of the transformer. Based on these requirements, we have developed a passive beam diagnostic instrumentation using a combination of a Chromox-6 scintillation screen and CCD camera. This paper describes details of the beam profile and position obtained from the CCD image with B = 0 T and B = 3 T, and for high and low intensity proton beams. A comparison is made with beam size obtained from multi-wires detector. Beam transmission efficiency through a collimator with a 4 mm diameter hole is measured by the toroids and CCD image of the scintillation screen. Results show that the transmission efficiency estimated from the CCD image is consistent with the toroid measurement, which enables us to monitor the beam transmission efficiency even in a high magnetic field environment.
 [http://dx.doi.org/10.1063/1.4808275]

I. INTRODUCTION

High intensity, low emittance muon beams are essential for the development of Muon Colliders and/or Neutrino Factories. Low emittance muon beams can be produced by ionization cooling.[1–7] This consists of passing muon beams through low-Z absorber material (H) to reduce all components of the momentum and replacing only the longitudinal component using RF cavities. At the same time, to keep the muon beam focused, both the absorbing material and RF cavity must be placed inside strong magnetic fields. One of the ionization cooling schemes under development at the MuCool Test Area (MTA) at Fermilab is a RF cavity filled with high pressure hydrogen gas. This technique has two advantages: first, the energy absorption and energy regeneration occur simultaneously rather than sequentially. Second, a higher RF gradient in an external magnetic field is achieved due to breakdown suppression by the Paschen effect. To investigate this technique, an experiment has been carried out at the MTA to study beam loading effects in a High Pressure RF (HPRF) cavity using a 400 MeV proton beam. Electrons are produced in the cavity through beam-induced ionization and consume a large amount of RF power. It has been shown[8] that the number of electrons produced per centimeter inside the cavity by each incident proton is ∼1600 at 100 atm hydrogen gas. For accurate measurement of the number of protons passing though the cavity, precise control of the beam intensity is an essential requirement. This has been done by putting collimators in front of the cavity.[9,10] In the present experimental setup, a 4 mm diameter hole collimator is placed in front of the cavity followed by another 20 mm hole diameter collimator as shown in Fig. 1.

Measurement of beam transmission efficiency through the collimators is an important element of the experiment and one of the objectives of this paper. The MTA is a flammable gas (hydrogen) hazard zone so no energized beam monitoring device can be used within 15 feet of the cavity due to safety reasons. It is to be noted that the toroids used as beam intensity monitor devices are made of ferrite material and, thus, when the magnetic field is turned on they do not work because of saturation. Looking into these requirements, we have developed a passive beam diagnostic instrument using a combination of a Chromox-6 scintillation screen and a CCD camera. Scintillation screens are widely used for beam profile monitoring in many particle accelerators.[11–22] Several decades of research on ceramic scintillators at various accelerator laboratories including CERN[14,21] has led to the use of Chromox-6 for beam profile measurement. We have chosen the Chromox-6 scintillation screen and the PixeLINK USB CCD camera. This camera needs electrical power and for safety reasons it is kept at a distance of more than 15 feet from the RF

[a)]On leave from Institute for Plasma Research, Bhat, Gandhinagar 382428, India. Electronic mail: mukti@fnal.gov.
[b)]On leave from Handong Global University, Pohang 791-708, South Korea.

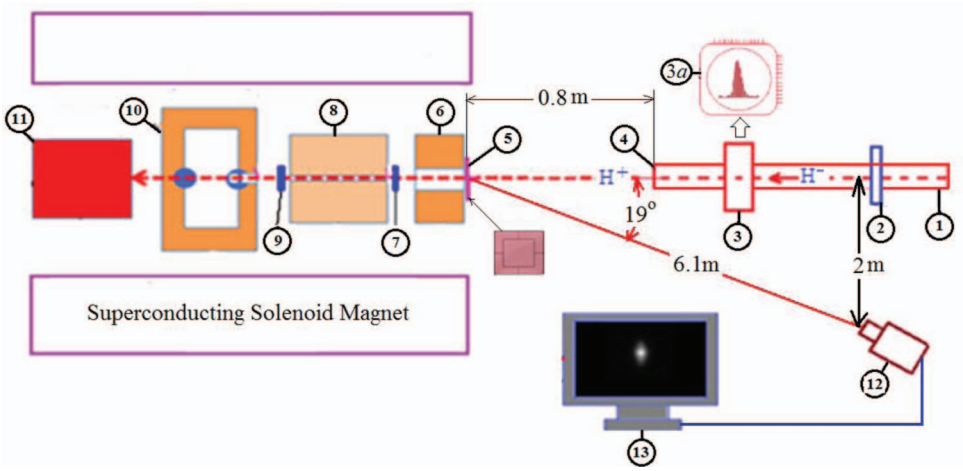

FIG. 1. Experimental setup at the Fermilab MuCool Test Area for the HPRF cavity test with the 400 MeV proton beam (not in scale). 1: Beam pipe, 2: Linac Toroid (LT), 3: Multi-wire detector, 3(a): Device (96 wires) inside flange, 4: Titanium window near end of beam pipe, 5: Chromox-6 scintillation screen, 6: First beam collimator (through hole diameter of 20 mm), 7: Up Stream (US) toroid, 8: Second beam collimator (through hole diameter of 4 mm), 9: Down Stream (DS) toroid, 10: HPRF cavity, 11: Beam absorber, 12: CCD camera, 13: Sample CCD image on PC.

cavity. The Fermilab Linac beam of species H^-, energy ~400 MeV, with a repetition rate of 1 macro pulse per min is used in the beam test experiment. The CCD image of the beam spot on the Chromox-6 scintillation screen is monitored online on a personal computer (PC) and quick online analysis (position of the beam on the screen) is done using the image processing software ImageJ[23] before the next pulse arrives within 1 min. This scheme guides the beam operator for tuning the beam. The CCD image shows that the beam is elliptical in shape and elongated vertically. The CCD images of the beam are viewed online and saved on the PC for post analysis. Saved image data are filtered from background noise and fitted with a Gaussian function. The average horizontal beam size (σ_x) is ~1.84 ± 0.03 mm and the vertical size (σ_y) is ~4.83 ± 0.18 mm. These should agree with the reference beam profile that is taken by a multi-wire detector located at a distance of ~1098 mm from the screen. Reference beam sizes are σ_x ~2.69 ± 0.19 mm and σ_y ~5.49 ± 0.23 mm. The larger beam size (in comparison to CCD image of beam) of the reference beam may be due to focusing of the beam or poor spatial resolution of the multi-wire, which is ~2 mm.

Beam transmission efficiency through the 4 mm hole collimator is measured by the toroid and the CCD image on the scintillation screen. Results show that for B = 0 T, the transmission efficiency measured by the toroids is ~21 ± 1.4% and by the CCD image is ~17.3 ± 0.8%. On the other hand for B = 3 T, the transmission efficiency from the CCD image is ~17.6 ± 0.6%. The salient feature of this paper is that the CCD image on a scintillation screen which is placed in air can be used for a quantitative estimation of the beam transmission through a narrow beam collimator placed in a high magnetic field where no other active beam diagnostic instrumentation works.

This paper is organized as follows: first an experimental setup of the HPRF beam test is described. Then analysis and results are discussed with high intensity and low intensity beam for B = 3 T and B = 0 T, respectively. Finally, conclusions are presented.

II. EXPERIMENTAL SETUP

Figure 1 shows the experimental setup. A negative hydrogen ion (H^-) beam of energy 400 MeV, 10 μs pulse length, intensity ~2×10^{12} protons per pulse (ppp) from the Fermilab Linear Accelerator (Linac) is used in this experiment. The H^- beam is sent through a beam pipe of 40 mm inner diameter and becomes a proton (H^+) beam after stripping off two electrons ($H^- \rightarrow H^+ + 2e$) in a titanium window (thickness 0.07 mm) placed near the end of the beam pipe. After passing through the window, the proton beam hits a Chromox-6 scintillation screen (size 40 mm × 40 mm × 1 mm) attached to the first collimator front end which is at a distance of 0.8 m from the titanium window. The beam image on the screen is viewed by a CCD camera placed at a distance of 6.1 m from the scintillation screen and 2 m from the axis of the beam pipe. The angular position of the CCD camera is 19°. Before entering the HPRF cavity (filled with 20–100 atm hydrogen gas), the beam passes through two co-axial cylindrical collimators made of stainless steel (SS 316L). The first has a 152.4 mm diameter, 100.6 mm length, with a through-hole diameter of 20 mm. The second collimator length is 203.2 mm, diameter is 152.4 mm, and has a through-hole diameter of 4 mm. In this arrangement, a well collimated beam is passed through the cavity. The beam intensity is monitored by two toroids. One [named here as the Up Stream (US) toroid] is placed in between the first and second collimator; the other [named here as the Down Stream (DS) toroid] is kept between the second collimator and the cylindrically shaped HPRF cavity (diameter 304.8 mm) made of stainless steel (SS 316L). The beam intensity data from both the US and DS toroids are saved on a PC at the same time for post analysis.

After traversing the cavity, the beam is finally dumped into a stainless steel solid cylindrical beam absorber of length

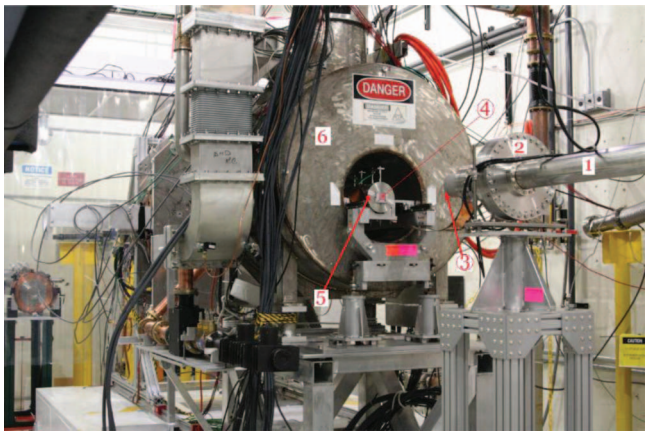

FIG. 2. Photograph of the experimental setup at the MuCool Test Area at Fermilab. 1: Beam pipe, 2: Multi-wire detector, 3: Titanium window, 4: Chromox-6 scintillation screen, 5: First beam collimator, 6: Superconducting solenoid magnet.

200.1 mm and diameter 152.4 mm. The Chromox-6 scintillation screen, collimators, toroids, HPRF cavity, and beam absorbers, all are placed inside a superconducting solenoid magnet which can produce a magnetic field of 3 T. When a 400 MeV proton beam hits the Chromox-6 scintillation screen, it emits light which is captured by the CCD camera.

To obtain a clear view of the Chromox-6 scintillation screen, the CCD camera is fitted with a telephoto lens of adjustable focal length ∼16–160 mm. The camera is controlled by software for online monitoring of the image, which is stored on a personal computer for post analysis. A reference grid of size 20 mm × 20 mm is marked on the screen surface which allows translating the number of pixels to millimeters. This arrangement provides a resolution of ∼7.1 pixels/mm. This reference grid is used for estimation of the beam center position (X_0, Y_0) with respect to the screen center that is precisely aligned to the collimator hole. A neutral density filter of attenuation ∼13% is used to avoid saturation of the CCD camera.

The photograph shown in Fig. 2 depicts various experimental components used for the HPRF cavity beam test at the MuCool Test Area at Fermilab with the 400 MeV proton beam transport line. In Subsections II A–II E brief descriptions are given for the beam parameters, Chromox-6 scintillation screen, CCD camera, multi-wire detector, and toroids.

A. Beam parameter

The energy of the H^- beam (after the titanium window it is converted to a H^+ beam) is 400 MeV, the average beam current is 36 mA, and the pulse length is 10 μs. The number of ppp is $\sim 2 \times 10^{12}$. The beam pulse repetition rate is 1 per min. Other beam parameters are listed in Table I.

B. Scintillation screen

Scintillation screens are widely used for measurement of charged particle beam profiles. In the last decade there has been significant development in technology for detection and efficient collection of light produced by scintillation materials.[11–22] The choice of scintillation material is based on the following properties.

TABLE I. Beam parameters.

Beam parameters	Value
Energy	400 MeV
Average beam current	36 mA
Species	H^-/H^+
Macro bunch length	10 μs
Micro bunch spacing	5 ns (200 MHz)
No. of micro bunch (10 μs/5 ns)	2000
Particle per macro bunch (particles per pulse)	$\sim 2 \times 10^{12}$
Particle per micro bunch (2×10^{12} /2000)	$\sim 1 \times 10^{9}$
Average charge	240 nC
Repetition rate	1 macro-bunch/min
Emittance, $\varepsilon_{95\%}$ (simulated)	10 mm-mrad

(a) *Conversion efficiency (Light yield)*: Conversion of kinetic energy of the charged particles into detectable light with a high scintillation efficiency which is defined as the average number of photoelectrons produced per eV input;
(b) *Emission spectra*: Emission light is matched to the optical system of the CCD camera in visible wavelength range (450 nm < λ < 700 nm);
(c) *Luminescence decay time*: Fast decay time is required for the observation of a variation of beam size;
(d) *Linearity*: This means light output is proportional to the incident particle flux over as wide a range as possible;
(e) High radiation hardness to prevent permanent damage;
(f) Good mechanical properties.

Various types of scintillation screens are used as beam monitoring devices in accelerator laboratories worldwide depending on the particle type and energy as reviewed by several authors.[16–18] Plastic scintillators[18] have low radiation hardness and, therefore, inorganic scintillation screens are used in beam diagnostic instruments.

Chromox-6 is 0.5% chrome doped in an alumina ceramic screen, i.e., Al_2O_3:Cr^{3+}. Its principle luminescence consists of two sharp lines (R lines) that arise from the transition from the lowest excited state to the ground state of Cr^{3+}. At room temperature these lines occur at 692.9 nm and 694.3 nm.[19,21] This screen is also Ultra High Vacuum (UHV) compatible and has good thermal stability, i.e., stable luminescence brightness (±15%) over the range from room temperature[24] to 450 °C. The screen also exhibits good linear response and high radiation resistance (10^{12} Ω-cm at 400 °C). A test has been done at CERN[25] and it showed that Chromox-6 scintillation screen withstood integrated relativistic proton fluxes of up to 10^{20} protons/cm^2. The ionization loss is ∼1 MeV/mm for ultra-relativistic protons.[22] Due to its robustness, it is often used in accelerator laboratories worldwide. Other salient features of the Chromox-6 screen are: higher melting point of ∼2000 °C, good thermal shock resistance, and good thermal quenching characteristics.[25] At GSI[26] in Germany, a systematic study of linearity of various scintillation screens has been

TABLE II. Properties of Chromox-6 scintillation screen.

Parameters	Value
Material: Al_2O_3 (Ref. 27)	99.4%
Cr_2O_3	0.5%
Color	Pink
Wavelength of luminescent light (nm) (when impacted by electron or protons)	691–694
Bulk density (g/cc)	3.85
Grain size (μm)	10–15
Specific heat, C_p (J/kg K) @ 20 °C (Ref. 28)	900
Thermal conductivity (W/m K) @ 100 °C	30
Melting point (°C)	2000
Max. operating temperature (°C)	1600
Resistivity (Ω-cm) @ 400 °C	10^{12}
Attenuation co-efficient, α (mm^{-1}) @ 694 nm	0.8 ± 0.1
Starting sensitivity (viewed by CCD camera)	10^7–10^8 protons
Ionization loss (for ultra-relativistic protons) (MeV/mm) (Ref. 22)	~1

carried out using 295 MeV/u neon ions with 5×10^5 to 10^9 particles/pulse. Both results show that the Chromox-6 scintillation screen has good response in linearity.

We have selected the Chromox-6 scintillation screen for measurement of the 400 MeV proton beam profile with both B = 0 T and B = 3 T. It was procured from Morgan[27] Technical Ceramics, UK. Various properties of the Chromox-6 scintillation screen are shown in Table II. It is to be noted that the screen is installed in air.

C. CCD camera

The principle spectrum of the emitted light from the Chromox-6 scintillation screen at room temperature consists of two sharp lines at wavelengths of 692.9 nm and 694.3 nm. Thus, the optical detector must have maximum sensitivity at these wavelengths. Normal CCD cameras have maximum sensitivity at these wavelengths. A PixeLINK CCD camera[29] (Model: PL-B955, USB 2.0) from Edmund Optics, USA was used for capturing the beam image on the Chromox-6 scintillation screen. The camera was set to have identical resolution in both the horizontal and vertical direction without a skew component. The spatial resolution of the CMOS in the CCD is 4.65 μm × 4.65 μm square pixels. The number of active pixels is 1392 (H) × 1040 (V) which corresponds to the CCD sensing area of 6.5 mm (H) × 4.8 mm (V). To obtain a sharp and clear image on the scintillation screen, a telephoto lens with adjustable focal length of ~16–160 mm is attached to the CCD camera. The estimated horizontal angular fields of view are 22.96°–2.32° and vertical fields of view are 17.06°–1.71° for this range of focal lengths. Figure 1 shows the location of the CCD camera that is kept in air at a distance of 6.1 m away from the screen. With this optical arrangement the viewing area at the scintillation screen location is 245.58 mm × 184.18 mm which is larger than the screen viewing area of 40 mm × 40 mm. To overcome the saturation of the CCD, we used a Neutral Density (ND) filter from Edmund Optics, USA with the specification of 0.9 OD M72.0 × 0.75″ where 0.9 indicates an attenuation of $\sim 10^{-0.9} \approx 13\%$ and M72.0 × 0.75″ represents the dimension of the mounting thread. The beam image is recorded at a frame rate of 10 fps (frame per second).

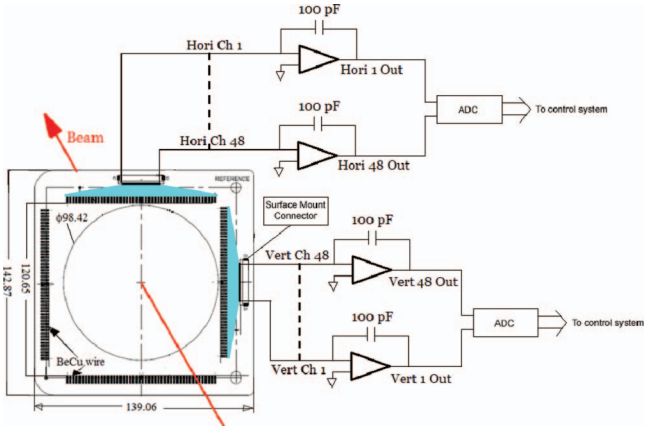

FIG. 3. Schematic diagram of a multi-wire detector and corresponding integrator channels. The solid state switches that control integration timing and reset are not shown for the sake of simplicity.

D. Multi-wire detector

In order to measure the reference beam profile and to tune the beam during operations, several multi-wire detectors are used in MTA beam line. One such multi-wire detector that is the closest beam profile monitor to the screen installed at the end of beam pipe is shown in Fig. 2. This consists of a ceramic frame (Alumina 96) of size 139.06 mm × 142.87 mm (shown in Fig. 3) assembled with 96 wires in two planes (horizontal and vertical) of 2 mm spacing to cover an area of 109.11 mm × 109.11 mm. Each wire has a diameter of 50 μm and is made of Beryllium Copper (BeCu). In the horizontal plane 48 wires are connected to a surface mount connector and the remaining 48 wires in the vertical plane are connected to another surface mount connector shown in Fig. 3. This detector operates in the beam line vacuum of $\sim 1.33 \times 10^{-9}$ mbar.

Parameters of the multi-wire detector are shown in Table III. The charge on the wires is measured by a scanner with 96 inputs designed by the Fermilab Control group. Forty eight inputs are connected to a horizontal vacuum feedthrough to measure the horizontal beam profile and the remaining 48 are connected to a vertical vacuum feedthrough for vertical beam profile measurement. Each input goes to its own analog integrator of type ACF2101 or IVC102 (both by TI/Burr-Brown). Each wire is model as a current source. The charge supplied by the incident beam (current source) accumulates on a capacitor and, thus, turns into a voltage. The voltages are then read out by an Analog-to-Digital Converter (ADC). A 100 pF capacitor with a 50 ms integration time is used. Saturation in the wire is detected by an analog comparator which sets the threshold voltage to be 0–10 V in our case.

E. Toroidal current transformer (Toroid)

At the MTA beam line, the intensity of the 400 MeV (H^-/H^+) beam is measured by several toroids. This system

TABLE III. Parameters of multi-wire detector.

Parameters	Value
Diameter of the wire	50 μm
Spacing	2 mm
Length of the wires	120.65 mm
Number of wires in:	
Horizontal plane	48
Vertical plane	48
Material	Beryllium Copper (BeCu)
Tension	0.78 N
Signal wires	Kapton isolated
Insulation (frame)	Alumina 96
Vacuum performance	1.33×10^{-9} mbar
Maximum power deposited on a wire	0.34 μW/mm^2

consists of toroidal ferrite magnetic core with wire wrapped around it which acts as a secondary winding of the transformer and the passing beam is the primary winding of single turn. These beam intensity monitors are placed at different locations. Three Linac toroids installed in the MTA beam line are manufactured by Pearson Electronics. The primary beam intensity is measured by Linac toroid (LT) placed around the beam pipe (shown in position 2 in Fig. 1). Inside the SC magnet, two additional toroids are installed. One of them (US) is placed between the first and second collimators shown in Fig. 1 at position 7. The other (DS) is placed just after the second collimator as shown in position 9 in Fig. 1. Both US and DS toroids are made of manganese zinc ferrite cores manufactured by Fair-Rite Products Corp. The US toroid has a single core wound with five turns of plastic coated copper wire connected to a BNC connector. The DS toroid has three cores wound with five turns of plastic coated copper wire connected with a BNC connector. Each toroid is placed in an aluminum housing to provide shielding and allows easy mounting. To minimize the effect of image currents, a small annular gap is made inside the housing. Calibrations of the toroids are performed and the inductances are measured. Due to very limited space available inside the superconducting magnet in which all experimental components are placed (Fig. 1), an *in situ* calibration could not be performed. Instead, the calibrations are performed by using a wire and resistors to make a closed circuit, effectively creating a single turn primary winding. A function generator is connected and a 8.72 V, 100 kHz square wave is sent through the primary winding while the response of the toroid along with the function generator signal is measured on an oscilloscope. The resistor is changed in order to vary the primary current. The measured time constant and inductance are 4.15 μs and 207.5 μH, respectively. A 50 Ω resistor is used in an oscilloscope and the current in the primary (I_p) is 17.4 mA. Thus, the current in the secondary is obtained from the expression, $I_s = (N_p/N_s)I_p \sim 3.48$ mA, where N_p is the number of turns in the primary (=1), and N_s is the number of turns in the secondary (=5). The estimated output signal across the secondary is 174 mV. The measured output signal in the oscilloscope is 179 mV which is 2.7% higher than that estimated. All toroid data are available on a pulse to pulse basis and saved on a PC in the form of number of ppp for post analysis.

III. RESULTS AND ANALYSIS

A CCD camera is used to record the image of the scintillation light emitted by the screen under irradiation of the 400 MeV proton beam. Then the image data are transferred to the PC for online monitoring and post analysis. Both image capture and control of the camera are done by PixeLINK Capture OEM software.[29] Via the display panel various parameters, e.g., camera exposure time, gain, etc., are controlled during capturing of the image. We used an exposure time of 100 ms and a gain of 5.26 dB. A trigger circuit is used to synchronize the arrival of the beam pulse with the CCD camera. For each beam pulse, the image of the beam is saved on the PC either in a video file (.avi) or an image file (.bmp) format for offline analysis. The intensity of the 400 MeV H^- beam is measured by LT and the reference beam profile is measured by the multi-wire detector installed close to the end of the beam pipe. After exiting the titanium window (position 4 in Fig. 1) the H^- beam becomes a proton beam (H^+) and the CCD image of the proton beam is captured while passing through the Chromox-6 scintillation screen. Transmission through the collimators is measured by US and DS toroids at B = 0 T. The results of these beam monitoring devices are described in Subsections III A–III C.

A. Multi-wire data analysis

A multi-wire detector is used for measurement of the Linac beam profile. Data are filtered from background noise and Gaussian fits are done to compute the beam width. Horizontal and vertical beam profiles are shown in Figs. 4(a) and 4(b), respectively. It is to be noted that center wires (which measure the maximum beam intensity) in both profiles show saturation. This is due to the fact that a 100 pF capacitor is used in the integrator and the offset voltage is set at 0–10 V. When the Linac beam intensity is $\sim 2 \times 10^{12}$ H^- ions/pulse, the estimated voltage at the center wire is ~9.6 V. The beam is negative hydrogen ions (H^-), so additional outer electrons boil off of the surface of the wire, along with secondary emission electrons. This leads to a voltage above the value of the offset voltage and saturation occurs. To overcome this saturation effect a higher value of capacitor shall be used in the integrator during the next beam operation.

The multi-wire detector has a spatial resolution of 2 mm. The beam is more focused in the horizontal direction and fewer wires measure the core of the beam. This introduces more error in the measurement. On the other hand, in the vertical direction the beam is much wider and more wires are available for the measurement of the vertical beam profile. Besides this, each multi-wire profile shows a large tail as shown in Fig. 4. This is due to charge accumulation in the ceramic frame of the detector which causes another source of error. Average values of σ_x and σ_y without magnetic field (B = 0 T) are $\sim 2.69 \pm 0.19$ mm and 5.49 ± 0.23 mm, respectively, as shown in Fig. 5.

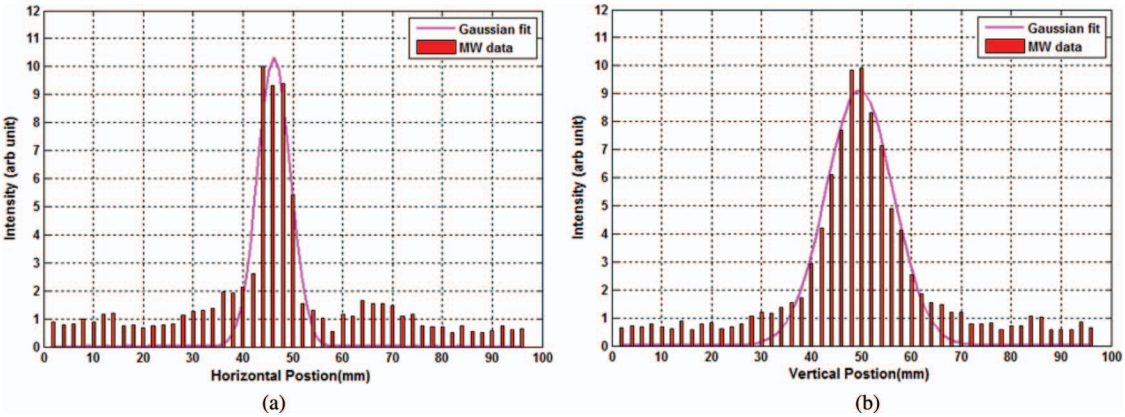

FIG. 4. H^- beam profiles obtained from multi-wire detector raw data and Gaussian fits: (a) horizontal beam profile (b) vertical beam profile. Note that H^- carries negative charge and all signals obtained from wires are negative but in this plot we took absolute values of the signals.

B. CCD beam image data analysis [beam profile, beam width (σ_x, σ_y), and beam center (X_0, Y_0)]

1. High intensity beam

Figure 6 depicts a sample of the CCD image of the 400 MeV proton beam ($\sim 2 \times 10^{12}$ ppp) on the Chromox-6 scintillation screen. The screen center is aligned with the center of the collimator holes (through which the beam axis passes) with an accuracy of 0.6 mm. The coordinate system used for image analysis is also shown. The CCD image has an elliptical cross section which indicates the beam is more focused horizontally and has a large tail in the vertical direction. Quantitative analysis of the beam image was performed by IMAGEJ[23] and Wolfram Mathematica.[30] After background noise subtraction, we obtained horizontal and vertical beam profiles which are shown in the top and right hand side (RHS) of Fig. 6. From the Gaussian fits of the horizontal and vertical beam profiles, we estimated the horizontal beam width (σ_x) and vertical beam width (σ_y), respectively.

Figure 7 depicts the values of σ_x (circles) and σ_y (triangles) estimated from the CCD image analysis. This shows that the average value of σ_x is $\sim 1.83 \pm 0.03$ mm and σ_y is $\sim 4.88 \pm 0.23$ mm for B = 0 T (shot number 1–91). On the other hand, in the case of B = 3 T (shot number 92–167), the value of σ_x is $\sim 1.86 \pm 0.03$ mm and σ_y is $\sim 4.78 \pm 0.06$ mm. The statistical error in σ_y for B = 0 T is higher than B = 3 T. This may be due to the error in Gaussian fit of the asymmetric vertical beam profile and instability in the Linac beam particularly for B = 0 T case. The overall average values of σ_x and σ_y are 1.84 ± 0.03 mm and 4.83 ± 0.18 mm for the entire beam shots (shot number 1–167).

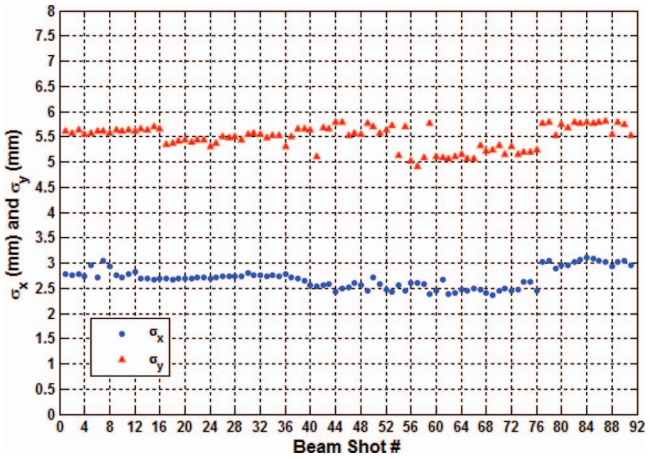

FIG. 5. Horizontal beam width (σ_x) and vertical beam width (σ_y) at different beam shot numbers obtained from multi-wire detectors.

Figure 8 illustrates the foot print of the beam center (X_0, Y_0) on the scintillation screen. The coordinates of collimator hole center are (20 mm, 20 mm) through which the beam axis passes. The CCD raw data (circles) indicate that the horizontal positions (X_0) of majority of the beam center have shifted left but the vertical positions (Y_0) are almost symmetric except for a few. Gaussian fitted data (triangles) show that the horizontal positions (X_0) of most of the beam centers have shifted left, whereas the vertical positions (Y_0) are shifted upward. This difference is due to the fact that the vertical beam profile is not symmetric (Fig. 6) and the Gaussian fit introduces some error in Y_0.

Figure 9 shows how the horizontal and vertical positions of the beam center varies with beam shots. Circles and up triangles indicate positions of X_0 and Y_0 which are obtained from the CCD raw data. Diamonds and down triangles are shown for the Gaussian fit data. Those beam centers that lie on a line passing through 20 at the Y axis (Fig. 9) are considered well centered. This shows that the center position of most of the beam is 20 ± 0.5 mm. A polynomial fit (4th order) of both the CCD raw data and Gaussian fit data shows the visual trend of variation.

2. Low intensity beam

During the experiment, the ion source current of the Linac is kept fixed and the maximum beam intensity is $\sim 2 \times 10^{12}$ ppp. It has been decided that the experiment can be performed with low beam intensity by passing the tail of the beam through a collimator hole. This has been obtained by displacing the beam center from the axis by changing the quadrupole magnet (installed in the MTA beam line) current. Figure 10 depicts a sample of the CCD image of low

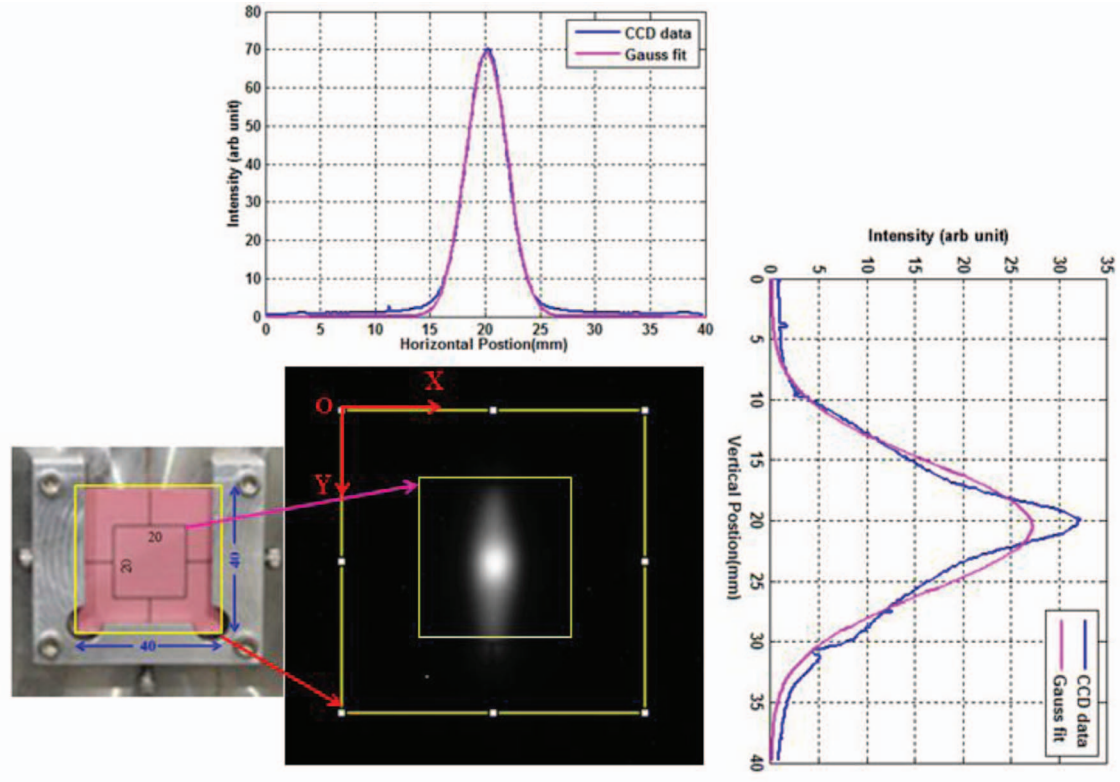

FIG. 6. CCD image of the 400 MeV, 36 mA, 10 μs pulse proton beam taken with the Chromox- 6 scintillation screen (40 mm × 40 mm × 1 mm) with an inner grid of size 20 mm × 20 mm. Origin of the coordinate is at the upper left corner. Both horizontal and vertical beam profiles and their Gaussian fits are shown separately. Acquisition time was 100 ms.

intensity beam with projected horizontal and vertical beam profiles. The beam center is displaced downward and toward the RHS from the center of the scintillation screen. Both horizontal and vertical beam profiles show an asymmetry. A Gaussian fit of the profile introduces a large error. Hence, information of the beam center and the width of the beam are not available. Nonetheless, a low intensity CCD image is used for the estimation of beam transmission through the collimator holes and a comparison has been made with the US and DS toroid data taking into account both conditions of B = 0 T and B = 3 T.

C. Beam transmission calculation

The main goal was to calculate the beam transmission efficiency through the first and second collimator holes from the CCD image on the screen. After subtracting the background noise, a 2D image is constructed using the Mathematica software, shown in Fig. 11. Integrating the volume under the 2D image would give the total number of emitted photons, which corresponds to the number of protons incident on the screen. We have assumed that the beta (β) function of the beam remains constant. A flow chart of the beam transmission

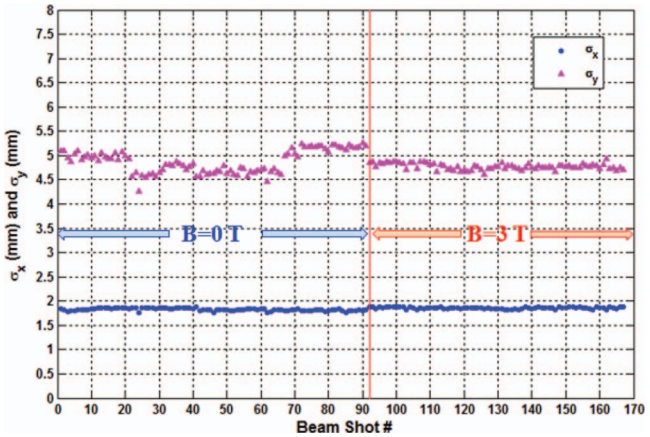

FIG. 7. Horizontal (σ_x) and vertical (σ_y) beam widths at different beam shots obtained from various days of beam operation. Beam shots 1–91 for B = 0 T and 92–167 for B = 3 T.

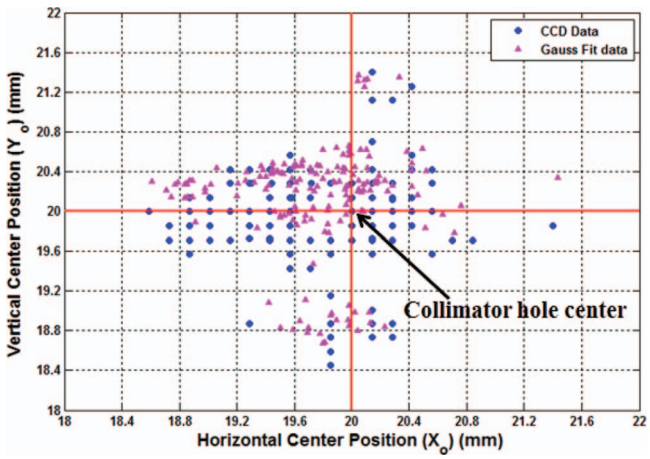

FIG. 8. Foot print of the horizontal (X_0) and vertical (Y_0) position of the beam center.

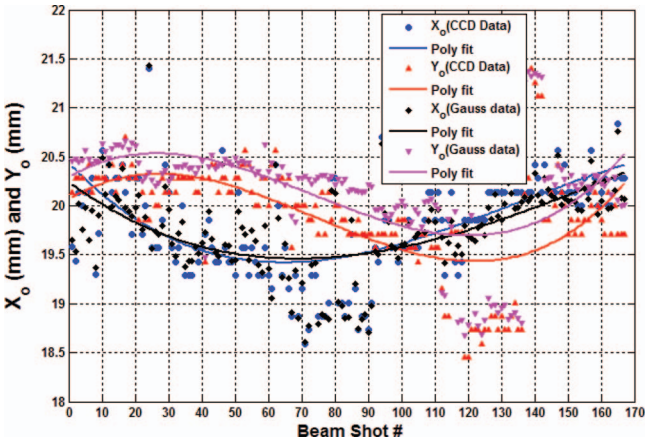

FIG. 9. Variation of horizontal (X_0) and vertical (Y_0) positions of the beam centers at different beam shots. Circles and up triangles indicate raw CCD image data. Diamonds and down triangles represent Gaussian fit data. Polynomial fits of both data show a visual trend in variation.

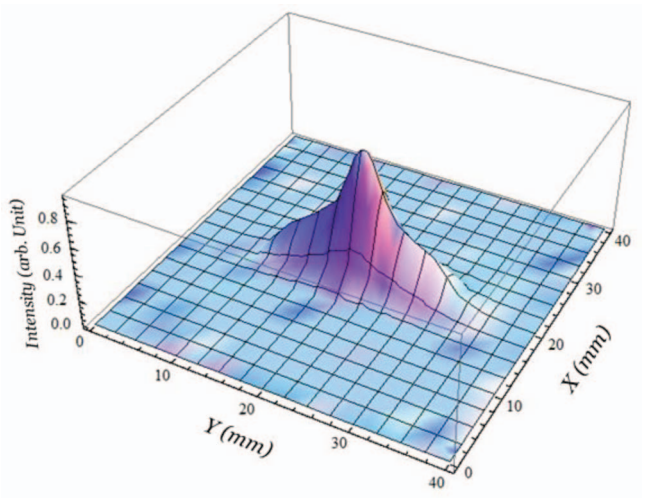

FIG. 11. Three-dimensional plot of CCD image on Chromox-6 scintillation screen.

calculation is shown in Fig. 12. First the CCD image (.bmp file) is imported in Mathematica with known X, Y coordinates and the 2D image is constructed. Integrating the volume over the 2D beam image (say I_1) gives the number of incident protons which can be measured by LT independently. Similarly, integration of the 2D image volume intercepted by a circle (say I_2) of diameter 20 mm (first collimator hole) and also integration of the 2D image volume intercepted by a circle (say I_3) of diameter 4 mm (second collimator hole) are calculated. The ratios, $I_2/I_1(=T_1)$ and I_3/I_1 $(=T_2)$, give the beam transmission efficiency through the first and second collimator, respectively. Further, LT $\times$ T_1 would give the fraction of the beam intensity passing through the first collimator hole.

We compare these intensity values with signals from the US toroid placed between the first and second collimators. It is to be noted that second collimator is placed 50 mm behind the first collimator. Thus, the intensity (LT $\times$ T_1) from the first

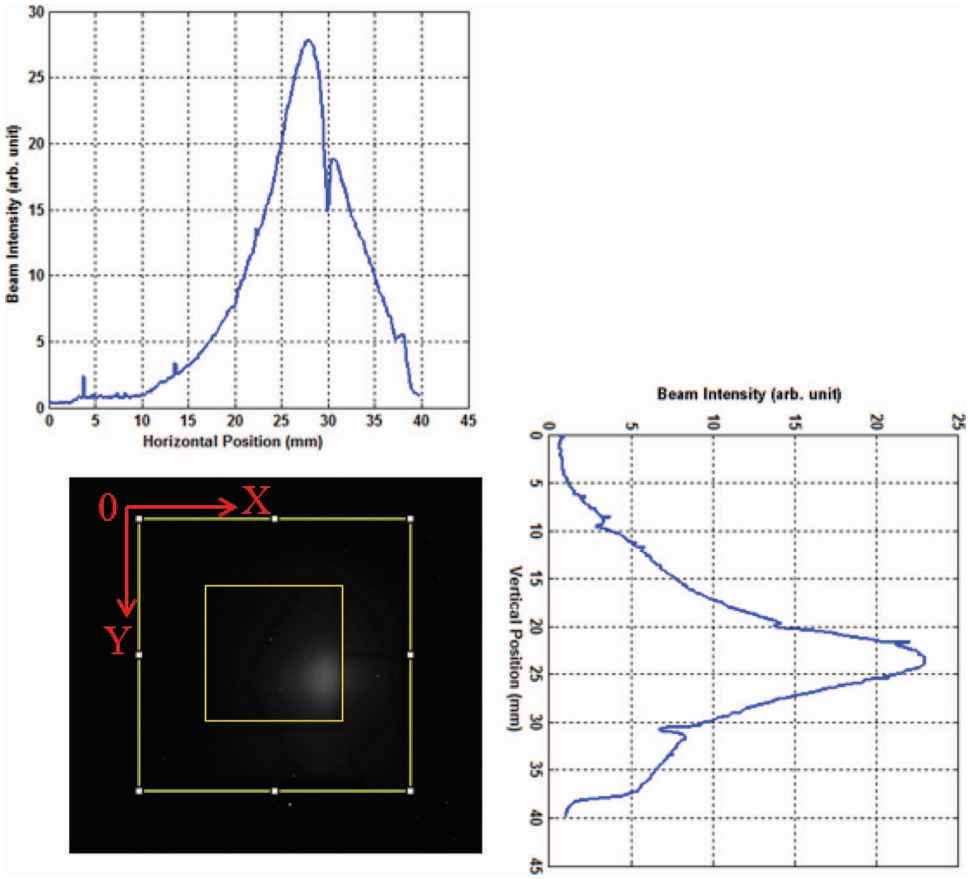

FIG. 10. CCD image and projected profiles of low intensity proton beam. The sharp deeps in the intensity plots are due to the reference grids.

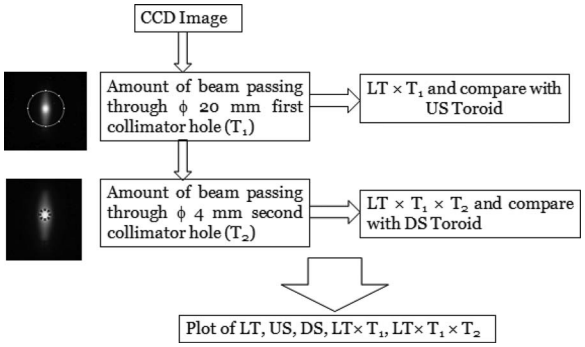

FIG. 12. Flow chart diagram for the calculation of beam transmission through first and second collimators, and comparison with Up Stream (US) and Down Stream (DS) toroids.

collimator is the incident intensity for the second collimator. Therefore, LT $\times$ T_1 $\times$ T_2 would give the amount of beam passing through the second collimator, which finally enters the HPRF cavity. We compare this value with signal from the DS toroid placed between the second collimator and HPRF cavity. Finally, comparison plots are made taking intensity values from the different measurements mentioned above.

The beam test experiment at the MTA has been done with four modes of operation, e.g., (i) high intensity without magnetic field, (ii) high intensity with a 3T magnetic field, (iii) low intensity without magnetic field, and (iv) low intensity with a 3 T magnetic field. Results of each mode of operation are described in Subsections III C 1–III C 4.

1. High intensity and without magnetic field (B = 0 T)

Figure 13 depicts the results of beam intensity measurement by various beam monitor systems used in the experiment at the MTA when the magnetic field is turned off (B = 0 T). This shows two distinct regions of intensity, e.g., shot numbers 1–41 (region I) and shot numbers 42–83 (region II). The average intensity measured by LT (circles) in these two regions is $\sim 2 \times 10^{12}$ ppp (pulse length of ~ 9.5 μs) and $\sim 1.5 \times 10^{12}$ ppp (pulse length of ~ 7.5 μs), respectively.

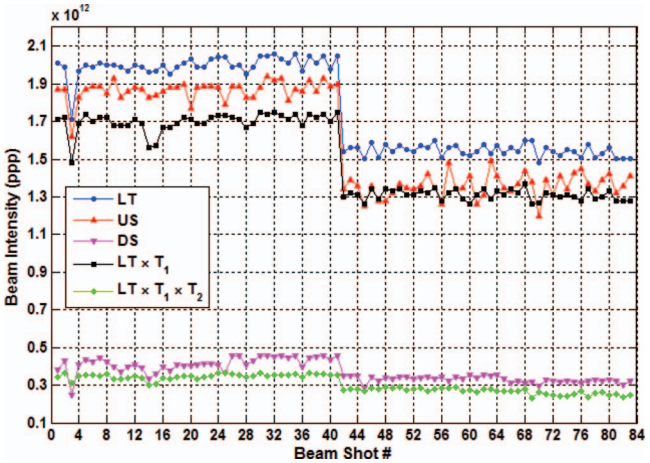

FIG. 13. Results of intensity measurements by various beam monitor devices for high intensity proton beam and B = 0 T. Toroid measurement data: circles (LT), up triangles (US toroid), and down triangles (DS toroid). CCD image analyzed data: at the exit of the first collimator (squares) and at the exit of the second collimator (diamonds).

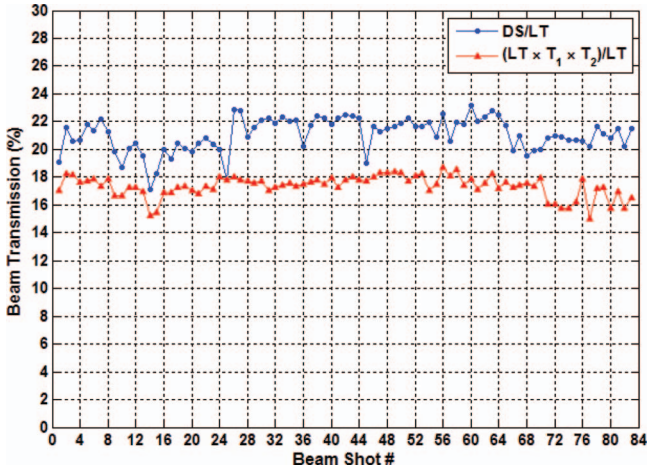

FIG. 14. Beam transmission through the second collimator at different beam shots for B = 0 T. Circles and triangles are measured data from toroids and CCD image analysis, respectively.

The intensity drop in region II is mainly due to the pulse length change in the Linac. It should to be noted that the Linac beam intensity is not constant due to variation of the ion source current and power supply ripple in various components (e.g., C-Magnets, Quadrupoles, etc.) used to steer the beam. In region I, the average intensity at the exit of the first collimator measured by the US toroid (up triangles) is $\sim 1.87 \times 10^{12}$ ppp and the CCD image estimated (LT $\times$ T_1) value (squares) is $\sim 1.70 \times 10^{12}$ ppp. At the exit of second collimator, the DS toroid value (down triangles) is $\sim 4.13 \times 10^{11}$ ppp and the CCD image analyzed (LT $\times$ T_1 $\times$ T_2) value (diamonds) is $\sim 3.46 \times 10^{11}$ ppp. On the other hand in region II, the average intensities measured by the US toroid and CCD image (LT $\times$ T_1) are $\sim 1.36 \times 10^{12}$ ppp and 1.31×10^{12} ppp respectively. Again, the DS toroid and CCD image (LT $\times$ T_1 $\times$ T_2) values are $\sim 3.30 \times 10^{11}$ ppp and 2.67×10^{11} ppp, respectively. This shows that the toroid and CCD image measurements are in good agreement. Results of beam transmission efficiency through the second collimator are shown in Fig. 14. Toroid measurement (circles) data show that the transmission efficiency (ratio of DS and LT) through the second collimator is $\sim 21 \pm 1.4\%$. On the other hand, CCD image analysis values (triangles) show the transmission efficiency [(LT $\times$ T_1 $\times$ T_2)/LT] through the second collimator is $17.3 \pm 0.8\%$. The difference between these two measurements may arise from systematic errors associated with the saturation of the scintillation screen for the high intensity proton beam. Moreover, another source of error would be quality of the image which depends on several factors, e.g., scattering and absorption of the beam by the screen, grain size of screen material, doped condition, and temperature of the screen.

2. High intensity and with magnetic field (B = 3 T)

During the experiments with the high intensity proton beam with B = 3 T, both US and DS toroids stop working due to saturation of the ferrite material used for the

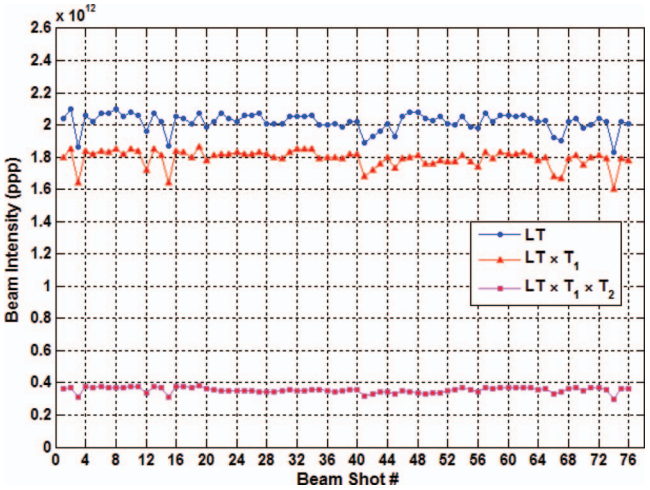

FIG. 15. Results of the intensity measurements by LT (circles) and CCD image of the screen indicated by triangles (exit of the first collimator) and squares (exit of the second collimator) for the high intensity proton beam and B = 3 T.

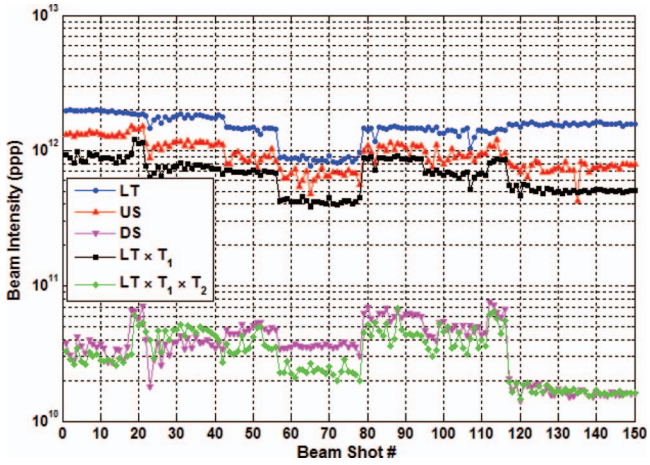

FIG. 17. Results of intensity measurements by beam monitoring devices at various beam shot number for low intensity proton beam and B = 0 T. Circles (LT), up triangles (US toroid), down triangles (DS toroid). CCD image analyzed intensity at the exit of the first collimator (squares) and the second collimator (diamonds).

transformer. The multi-wire detector was also not useful due to fringe fields generated by the magnet. In this situation a combination of the Chromox-6 scintillation screen and CCD camera was the only available beam intensity monitoring device. Moreover, simulation result[31,32] shows that the trajectory of the 400 MeV proton beam does not change when it passes through the collimator holes and HPRF cavity with the 3T magnetic field. No change in the shape of the image on the scintillation screen is noticed during the beam operation with B = 3 T. These observations indicate that we can use the scintillation screen to monitor the beam transmission efficiency through a narrow collimator in high magnetic field conditions. Figure 15 shows the results of intensity measurements for B = 3 T. LT data (circles) show that the incident average intensity is ~2.02 × 10^{12} ppp. Results of the CCD image analysis indicate that the mean intensity at the exit of the first collimator is ~1.79 × 10^{12} ppp (triangles) and at the exit of the second collimator is ~3.55 × 10^{11} ppp (squares). Beam transmission efficiency [(LT × T_1 × T_2)/LT] through the second collimator is ~17.6 ± 0.6% as shown in Fig. 16 which is consistent with the result for B = 0 T.

3. Low intensity and without magnetic field (B = 0 T)

Low beam intensity mode of operation is performed by passing the tail of the beam through the collimator hole, which is achieved by shifting the beam center from its axis. Figure 17 depicts the results of the low intensity beam measurements by various monitoring devices for B = 0 T. This shows that the beam intensity is not stable throughout the entire beam shots. Figure 18 depicts the beam transmission efficiency through the second collimator at different beam shots. It is interesting to note that the beam transmissions measured from the DS toroid (circles) and CCD image (LT × T_1 × T_2) estimated values (up triangles) vary consistently with respect to each other over the wide range of beam shots. In particular, for beam shots 117–150, the transmission efficiency

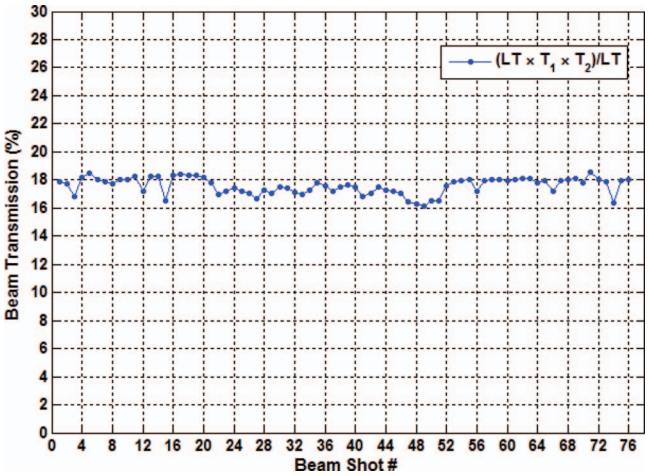

FIG. 16. Beam transmission efficiency through the second collimator at various beam shots for high intensity proton beam and B = 3 T.

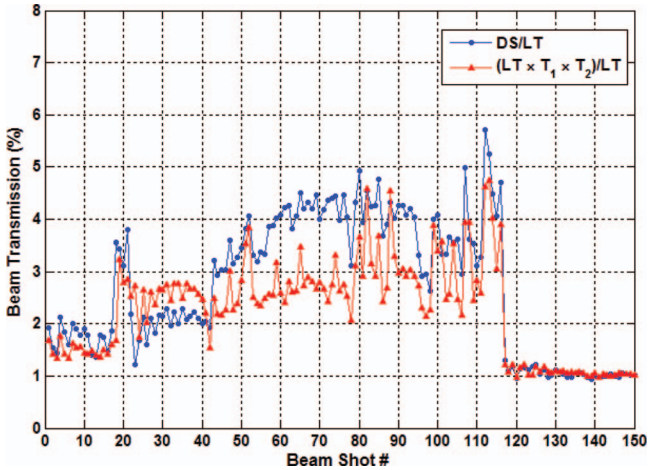

FIG. 18. Beam transmission through the second collimator versus beam shot number, obtained from toroid measurements (circles) and CCD image analysis (triangles) for low intensity and B = 0 T.

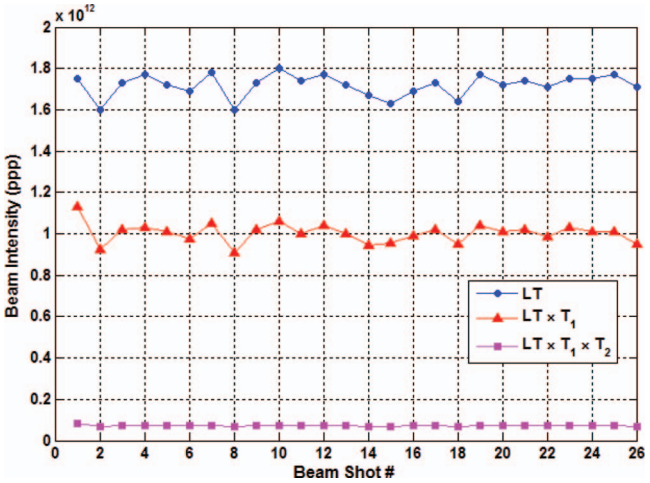

FIG. 19. Results of intensity measurements for low intensity proton beam and B = 3 T. LT (circles), and CCD image estimation at the exit of the first collimator (triangles) and at the exit of the second collimator (squares), respectively.

is ∼1.05 ± 0.08% from DS/LT and ∼1.07 ± 0.06% from (LT × T_1 × T_2)/LT, respectively.

4. Low intensity and with magnetic field (B = 3 T)

Figure 19 shows the results of the intensity measurements by the LT, and CCD image estimated values at the exit of the first collimator and also at the exit of the second collimator for the low intensity proton beam with B = 3 T magnetic field. The average incident intensity (circles) is ∼1.7 × 10^{12} ppp. At the exit of the first collimator (triangles) the beam intensity is ∼1 × 10^{12} ppp and at the exit of the second collimator (squares) is ∼1.2 × 10^{11} ppp.

Figure 20 shows the results of beam transmission efficiency through the second collimator obtained from the CCD image on screen. The average transmission efficiency is ∼4.19 ± 0.12%. It is to be noted that we have very limited data available for low intensity and B = 3 T. In the next beam test more data shall be acquired and results shall be reported elsewhere.

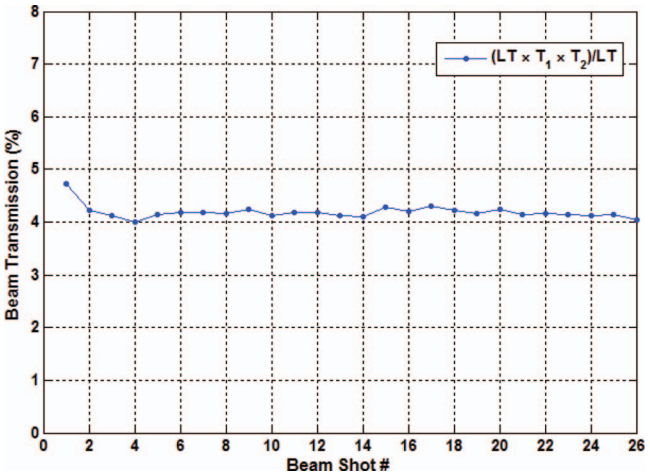

FIG. 20. Beam transmission efficiency through the second collimator for low intensity proton beam and B = 3 T.

IV. CONCLUSIONS

In the MuCool Test Area at Fermilab, the HPRF cavity experiments have been done with high and low intensity proton beam (400 MeV, ∼2 × 10^{12} ppp, 10 μs pulse length) with B = 0 T and B = 3 T to study the beam loading effect in the Muon Accelerator R&D program, USA. It has been observed that when this energetic proton beam passed through a RF cavity pressurized with hydrogen gas, it produced electrons. These ionized electrons consume RF power inside the cavity. Thus, accurate measurement of the proton beam intensity entering the cavity is an essential requirement of this experiment. A well collimated proton beam passing through the cavity is produced by placing a collimator of 4 mm diameter hole. The MTA is a flammable gas (hydrogen) hazard zone, hence no energized beam monitoring device can be used. Toroids are used (for B = 0 T) as beam intensity monitoring systems but they do not work at B = 3 T due to the saturation of the ferrite material. Another requirement of this experiment was an online viewing of the beam position so that the operators can tune the beam to confirm maximum beam transmission through the HPRF cavity. Considering these requirements, we have developed a passive beam diagnostic instrument using a combination of Chromox-6 scintillation screen (kept in air) and CCD camera. In this paper, we have demonstrated that the CCD image on a scintillation screen can be used for a quantitative measurement of the beam transmission efficiency even in a high magnetic field (B = 3 T) environment. It is to be noted that the CCD image estimated values of σ_x and σ_y are almost the same for both cases of B = 0 T and B = 3 T. This shows that the shape of the beam does not change significantly while passing through the collimator for B = 3 T, which is in agreement with beam optics simulations.[31,32]

For the high intensity and B = 0 T case, the average beam transmission efficiency through the second collimator obtained from the toroid measurement is ∼21 ± 1.4%, whereas the CCD image analysis shows it is ∼17.3 ± 0.8%. Furthermore for B = 3 T, toroids stop working but the scintillation screen works fine, and the CCD image estimated value of transmission efficiency is ∼17.6 ± 0.6%. In the case of low intensity and B = 0 T, toroid measurement data show the maximum transmission efficiency through the second collimator is ∼4.13 ± 0.30% and minimum is ∼1.05 ± 0.08%. On the other hand, the CCD image estimated values of maximum and minimum intensity are ∼3.20 ± 0.71% and 1.07 ± 0.06%. Furthermore, for low intensity beam and B = 3 T case, the CCD image estimated transmission efficiency is ∼4.19 ± 0.12%.

A simulation calculation[31] using G4beamline[33] computer code with a proton beam of σ_x = 1.67 mm and σ_y = 3.88 mm shows that the transmission efficiency through the 4 mm diameter collimator is 47%. Using these values of σ_x and σ_y in a Mathematica program developed for CCD image analysis we obtain a transmission efficiency of 55%. This benchmark calculation shows simulation and measurements are in reasonable agreement.

ACKNOWLEDGMENTS

Authors wish to thank C. Johnstone, G. Koizumi, J. Volk, M. Popovic, G. R. Tassotto, D. P. Schoo, M. Yang, D. R. Mcarthur, S. Geer, T. Sen, Fermilab Accelerator Division (AD), and Main Control Room (MCR) staff for various help during experiment. This work was supported by the Fermi Research Alliance, LLC under Contract No. De-AC02-07CH11359 with the United States Department of Energy (DOE).

[1]J. Monroe, P. Spentzouris, V. Balbekov, P. Lebrun, G. Penn, C. Kim, E. S. Kim, and D. M. Kaplan, Phys. Rev. ST Accel. Beams **4**, 041301 (2001).
[2]D. M. Kaplan, Nucl. Instrum. Methods **A453**, 37 (2000).
[3]R. Raja, *Muon Collider – Status and Physics Prospects*, FERMILAB-Conf-99/329.
[4]S. Geer and R. Raja, "Workshop on physics at the first muon collider and at the front end of the muon collider," AIP Conf. Proc. **435**, 3–855 (1998), http://ppd.fnal.gov/conferences/femcpw97/plenary/talks.html
[5]D. Neuffer and R. Palmer, "Progress towards a high energy high luminosity $\mu^+\mu^-$ collider," AIP Conf. Proc. **356**, 344 (1996).
[6]A. N. Skrinsky and V. V. Parkhomchuk, Sov. J. Part. Nucl. **12**, 223 (1981).
[7]D. Neuffer, AIP Conf. Proc. **156**, 201 (1987).
[8]K. Yonehara, "HPRF beam tests," MAP Weekly Meetings, 23 September 2011, https://indico.fnal.gov/conferenceDisplay.py?confId=4661.
[9]M. Chung, A. Jansson, A. Moretti, A. Tollestrup, K. Yonehara, and A. Kurup, in *Proceedings of IPAC, Kyoto, Japan* (2010), p. 3494.
[10]A. V. Tollestrup, M. Chung, and K. Yonehara, *Handbook for Gas Filled RF Cavity Aficionados*, Version 1.01, Fermilab TM-2430-APC (2009).
[11]B. Walasek-Hohne, *Proceedings of DIPAC 2011, Hamburg, Germany* (2011), p. 553.
[12]E. Gutlich, P. Fork, W. Ensinger, and B. Walasek-Hohne, IEEE Trans. Nucl. Sci. **57**, 1414 (2010).
[13]J. Harasimowicz, L. Cosentino, P. Finocchiaro, A. Pappalardo, and C. P. Welsch, Rev. Sci. Instrum. **81**, 103302 (2010).
[14]E. Bravin, "Scintillating screens use at CERN," in *Proceedings of the Workshop on Scintillating screen applications in beam diagnostics, GSI, Darmstadt, Germany* (2011), http://www-bd.gsi.de/ssabd.
[15]P. Strehl, *Beam Instrumentation and Diagnostics* (Springer, 2006), p. 120.
[16]R. Jung, G. Ferioli, and S. Hutchins, in *Proceedings DIPAC, Mainz, Germany* (2003), p. 10.
[17]M. J. Weber, J. Lumin. **100**, 35 (2002)
[18]G. F. Knoll, *Radiation Detection and Measurement* (John Wiley & Sons Inc., 2000), p. 219.
[19]D. Jimenez-Rey, B. Zurro, K. J. McCarthy, G. Garcia, and A. Baciero, Rev. Sci. Instrum. **79**, 10E516 (2008).
[20]K. J. MacCarthy, J. G. Lopez, F. M. Hernandez, B. Zurro, A. Baciero, and M. A. Respaldiza, J. Nucl. Mater. **321**, 78 (2003).
[21]T. Lefevre, C. Bal, E. Bravin, S. Burger, B. Goddard, S. Hutchins, and T. Renaglia, in *Proceedings of DIPAC, Venice, Italy* (2007), p. 132.
[22]L. Ludovici, UA9 London meeting (2012), http://indico.cern.ch/getFile.py/access?contribId=3&resId=0&materialId=slides&confId=188663.
[23]W. S. Rasband, ImageJ, U.S. National Institute of Health, Bethesda, Maryland, USA, http://rsb.info.nih.gov/ij (1997–2010).
[24]C. D. Johnson, "The development and use of alumina ceramics fluorescent screen," European Laboratory for Particle Physics Report, CERN/PS/90-42(AR).
[25]A. Aryshev, T. Aumeyr, G. A. Blair, S. T. Boogert, G. Boorman, A. Bosco, L. Corner, A. E. Dabrowski, L. Deacon, B. Foster, A. Gillespie, E. B. Holzer, S. Jamison, P. Karataev, T. Lefevre, K. Lekomtsev, M. Olvegard, S. Mallows, M. Micheler, L. Nevay, M. Sapinski, S. Smith, L. Soby, R. Walczak, C. Welsch, and M. Wendt, CLIC Conceptual design report on Beam Instrumentation, http://project-clic-cdr.web.cern.ch/project-CLIC-CDR/Drafts/Beam_Instrumentation_v19.pdf.
[26]K. Renuka, W. Ensinger, C. Andre, F. Beeker, P. Forck, R. Haseitl, A. Reiter, and B. Walasek-Hohne, "Transverse beam profile monitoring using scintillation screen for high energy ion beams," in *Proceedings of Beam Instrumentation Workshop, Newport, VA, USA*, *TUPG022* (2012).
[27]See www.morgantechnicalceramics.com for Morgan Technical Ceramics.
[28]U. Raich, "Instrumentation in small low energy machines," in *Proceedings of DIPAC, Lyon, France*, *ITMM01* (2005).
[29]See www.PixeLINK.com for PixeLINK website.
[30]See www.wolfram.com for Wolfram Research, Inc. USA.
[31]A. Tollestrup, "Data for collimator in MTA," (private communication).
[32]M. Leonova, "MTA beam line simulation," (private communication).
[33]See http://www.muonsinc.com/muons3/G4beamline for G4beamline, Muons, Inc.